Ministero dell'Università e della Ricerca

FIS

POLITECNICO MILANO 1863 | DEPARTMENT OF ENERGY

Numerical investigation of bubble columns with ionic liquids for CO_2 absorption

Vitor A. Regert dos Santos, Nicolò Varallo, Giorgio Besagni

Department of Energy, Politecnico di Milano · AURIGA project

Why ionic liquids in bubble columns?

Hard-to-abate emissions
Cement, steel, chemicals and refining cannot be decarbonized by electrification alone.

Bubble columns
Simple construction, no moving parts, excellent heat and mass transfer performance.

Ionic liquids
Negligible vapour pressure, thermal stability and tunable physicochemical properties.

The gap
CFD closures are calibrated on air–water; the IL here is ≈90× more viscous, so their transferability is unverified.

Objective
Assess the drag, bubble-induced-turbulence and mass transfer closures of the Euler–Euler framework in one high-viscosity system, against measured gas holdup and the empirical correlations.

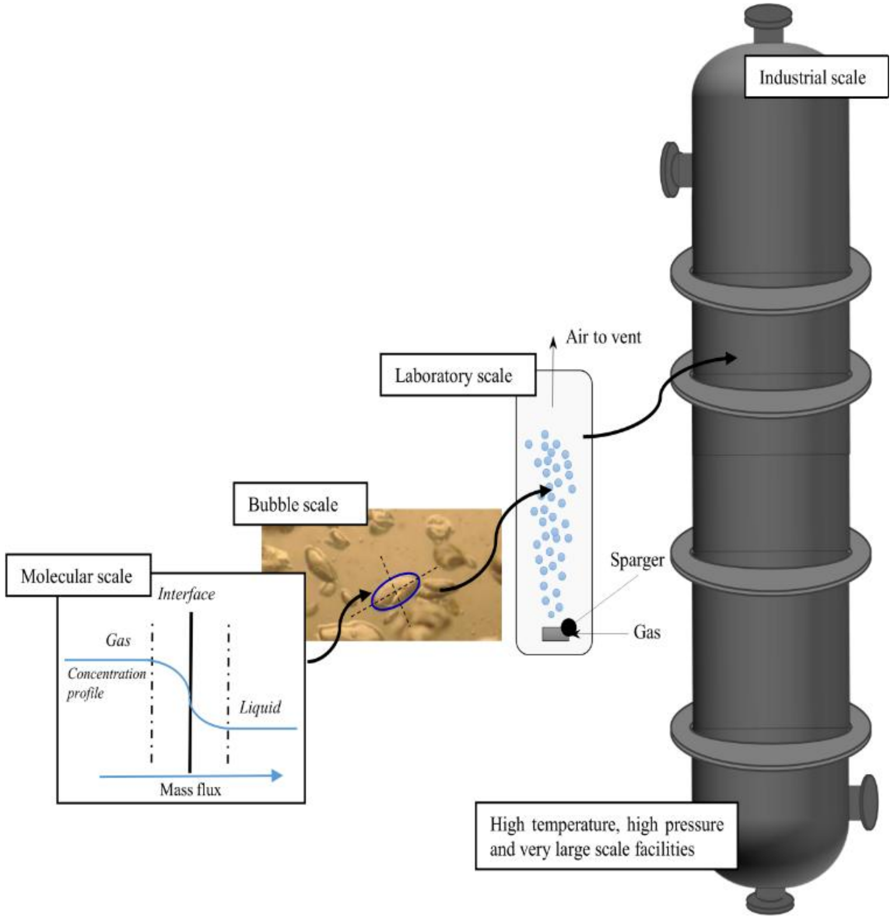

Mass transfer spans five orders of magnitude in length, from the diffusive film to the industrial reactor.

Euler–Euler transport equations and interphase forces

Phase continuity, momentum and the interphase momentum exchange — phase K ∈ {G, L}, one shared pressure field

$$\frac{\partial(\alpha_K \rho_K)}{\partial t} + \nabla \cdot (\alpha_K \rho_K \boldsymbol{u}_K) = \Gamma_K$$

$$\frac{\partial(\alpha_K \rho_K \boldsymbol{u}_K)}{\partial t} + \nabla \cdot (\alpha_K \rho_K \boldsymbol{u}_K \boldsymbol{u}_K) = -\alpha_K \nabla p + \nabla \cdot (\alpha_K \overline{\tau}_K) + \alpha_K \rho_K \boldsymbol{g} + \boldsymbol{M}_K + \Gamma_K \boldsymbol{u}_K$$

$$\boldsymbol{M}_K = \boldsymbol{F}_D + \boldsymbol{F}_L + \boldsymbol{F}_{\mathrm{VM}} + \boldsymbol{F}_{\mathrm{WL}} + \boldsymbol{F}_{\mathrm{TD}}$$

Drag F_D
Dong et al. (3)

Lift F_L
Tomiyama (8), Wellek (9)

Virtual mass F_{VM}
C_{VM} = 0.5 (12)

Wall lubrication F_{WL}
Antal et al. (10)

Turbulent dispersion F_{TD}
Burns et al. (11)

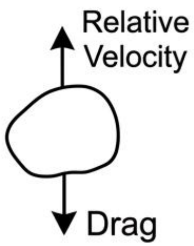

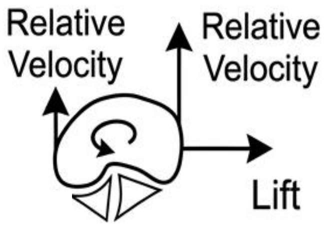

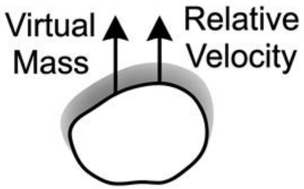

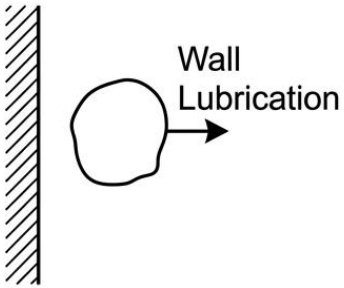

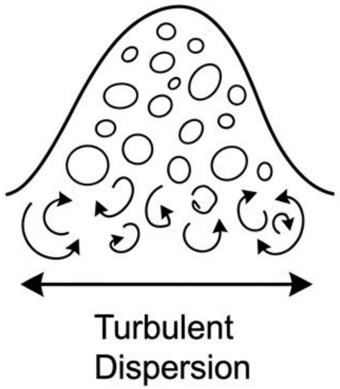

(3) *Dong H, Wang X, Liu L, Zhang X and Zhang S 2010 The rise and deformation of a single bubble in ionic liquids Chemical Engineering Science 65 3240–8*
(8) *Tomiyama A, Tamai H, Zun I and Hosokawa S 2002 Transverse migration of single bubbles in simple shear flows Chemical Engineering Science*
(9) *Wellek R M, Agrawal A K and Skelland A H P 1966 Shape of liquid drops moving in liquid media AIChE Journal 12 854–62*
(12) *Drew D, Cheng L and Lahey R T 1979 The analysis of virtual mass effects in two-phase flow International Journal of Multiphase Flow 5 233–42*
(10) *Antal S P, Lahey R T and Flaherty J E 1991 Analysis of phase distribution in fully developed laminar bubbly two-phase flow International Journal of Multiphase Flow 17 635–52*
(11) *Burns A, Frank T, Hamill I and Shi J-M 2004 The Favre averaged drag model for turbulent dispersion in Eulerian multi-phase flows Conf. on Multiphase Flow ICMF2004 vol 392*

Momentum source — drag coefficient and the swarm correction

Drag force on the dispersed phase

$$\boldsymbol{F}_D = \frac{3}{4}\frac{C_D}{d_B}\alpha_G \rho_L |\boldsymbol{u}_r| \boldsymbol{u}_r, \quad \boldsymbol{u}_r = \boldsymbol{u}_G - \boldsymbol{u}_L$$

Swarm correction — Rusche & Issa (2000) ⑦

$$C_D = C_{D,\infty}\, f(\alpha_G), \quad f = \exp(k_1 \alpha_G) + {\alpha_G}^{k_2}$$

$k_1 = 3.64$, $k_2 = 0.864$ — corrects the single-bubble C_D for the presence of neighbor bubbles.

Dong et al. (2010) † ③
Fitted to single-bubble rise in ionic liquids; the only candidate with an explicit Morton-number dependence.

Ishii & Zuber (1979) ⑤
Regime-based (viscous / distorted / cap)

Tomiyama (1998) ⑥ and Schiller-Naumann (1935) ④
Calibrated on air–water

Only the drag closure is varied at this stage . Every other force is held fixed, so the gas-holdup discrepancy is attributable to C_D alone.

③ Dong H, Wang X, Liu L, Zhang X and Zhang S 2010 The rise and deformation of a single bubble in ionic liquids Chemical Engineering Science 65 3240–8
④ Schiller L and Naumann A 1935 Über die grundlegenden Berechnungen bei der Schwerkraftaufbereitung Zeitschrift des Vereins Deutscher Ingenieure 77 318–20
⑤ Ishii M and Zuber N 1979 Drag coefficient and relative velocity in bubbly, droplet or particulate flows AIChE Journal 25 843–55
⑥ Tomiyama A, Kataoka I, Zun I and Sakaguchi T 1998 Drag coefficients of single bubbles under normal and micro gravity conditions JSME International Journal Series B 41 472–9
⑦ Rusche H and Issa R I 2000 The effect of voidage on the drag force on particles, droplets and bubbles in dispersed two-phase flow

Species transport and mass transfer closures

Species transport and the interfacial source term

$$\frac{\partial(\alpha_K \rho_K Y^i)}{\partial t} + \nabla \cdot (\alpha_K \rho_K Y^i \boldsymbol{u}_K) = \nabla \cdot \left(D^i \nabla(\alpha_K \rho_K Y^i)\right) + \Gamma_{K^i}$$

$$\Gamma_{L\mathrm{CO_2}} = k_L a\, \rho_L \left(He^{\mathrm{CO_2}} Y_{G\mathrm{CO_2}} \frac{\rho_G}{\rho_L} - Y_{L\mathrm{CO_2}} \right)$$

Liquid side controls: the gas-side resistance is negligible for CO_2 in an ionic liquid.

Interfacial area — monodisperse

$$a = \frac{6\alpha_G}{d_B}$$

Closed by the Sauter mean diameter of the benchmark.

Higbie (1934) — penetration, slip-driven ⑯

$$k_L = 2\sqrt{\frac{D}{\pi t_E}}, \quad t_E = \frac{d_B}{\boldsymbol{u}_r}, \quad \boldsymbol{u}_r = |\boldsymbol{u}_G - \boldsymbol{u}_L|$$

Jajuee et al. (2006) — surface-renewal stretch ⑰

$$k_L = \sqrt{\frac{4D}{\pi}\sqrt{\frac{\epsilon}{\nu_L}}}$$

Li et al. (2020) — modified eddy cell ⑱

$$k_L = \sqrt{D\sqrt{\frac{\epsilon}{\nu_L} - \frac{2\sigma}{\rho_L \nu_L}\frac{d}{dt}(|\nabla \alpha_L| \alpha_L)}}$$

The distinction that matters

Higbie takes the exposure time from bubble-scale kinematics; Jajuee and Li take the renewal rate from the turbulence field, so they inherit the BIT closure.

⑯ *Higbie R 1934 The rate of absorption of a pure gas into still liquid during short periods of exposure University of Michigan*
⑰ *Jajuee B, Margaritis A, Karamanev D and Bergougnou M A 2006 Application of surface-renewal-stretch model for interface mass transfer Chemical Engineering Science 61 3917–29*
⑱ *Li W-L, Wang J-H, Lu Y-C, Shao L, Chu G-W and Xiang Y 2020 CFD analysis of CO_2 absorption in a microporous tube-in-tube microchannel reactor with a novel gas–liquid mass transfer model International Journal of Heat and Mass Transfer 150 119389*

Turbulence and bubble-induced turbulence

Turbulence is solved in the liquid only (k–ω SST ⑬); the bubbles enter it as extra source terms in the k and ω equations.

Ma et al. (2017) † — DNS-calibrated ⑭

$$S_{k\mathrm{BIT}} = \min(0.18\, Re_B{}^{0.23}, 1)\, \boldsymbol{F}_D \cdot (\boldsymbol{u}_G - \boldsymbol{u}_L)$$

$$S_{\epsilon\mathrm{BIT}} = 0.3\, C_D \frac{S_{k\mathrm{BIT}}}{\tau}, \quad \tau = \frac{d_B}{|\boldsymbol{u}_G - \boldsymbol{u}_L|}$$

The Re_{B} factor is a viscous damping: not all the drag work becomes resolved turbulent kinetic energy.

Rzehak & Krepper (2013) ⑮

$$S_{k\mathrm{BIT}} = \boldsymbol{F}_D \cdot (\boldsymbol{u}_G - \boldsymbol{u}_L)$$

$$S_{\epsilon\mathrm{BIT}} = C_{\epsilon B} \frac{S_{k\mathrm{BIT}}}{\tau}, \quad \tau = \frac{d_B}{\sqrt{k}}$$

$C_{\varepsilon B}$ = 1.0. Assumes complete conversion of the drag work — calibrated on air–water.

Conversion to the ω equation (both closures)

$$S_{\omega\mathrm{BIT}} = \frac{1}{C_\mu k} S_{\epsilon\mathrm{BIT}} - \omega \frac{S_{k\mathrm{BIT}}}{k}$$

C_μ = 0.09.

Why this matters downstream

The turbulence-based mass transfer closures scale as $k_{\mathrm{L}} \propto \varepsilon^{1/4}$, so any bias in the BIT source propagates directly into the predicted $k_{\mathrm{L}}a$ field. Ma's Re_{B} factor stays well below unity when Re_{B} = O(1), as it is in a 107 mPa·s liquid.

⑬ Menter F R, Kuntz M and Langtry R 2003 Ten years of industrial experience with the SST turbulence model Turbulence, Heat and Mass Transfer 4
⑭ Ma T, Santarelli C, Ziegenhein T, Lucas D and Fröhlich J 2017 Direct numerical simulation–based Reynolds-averaged closure for bubble-induced turbulence Physical Review Fluids 2 034301
⑮ Rzehak R and Krepper E 2013 Closure models for turbulent bubbly flows: a CFD study Nuclear Engineering and Design 265 701–11

The case study — a CO_2 / [BMIM][BF_4] bubble column

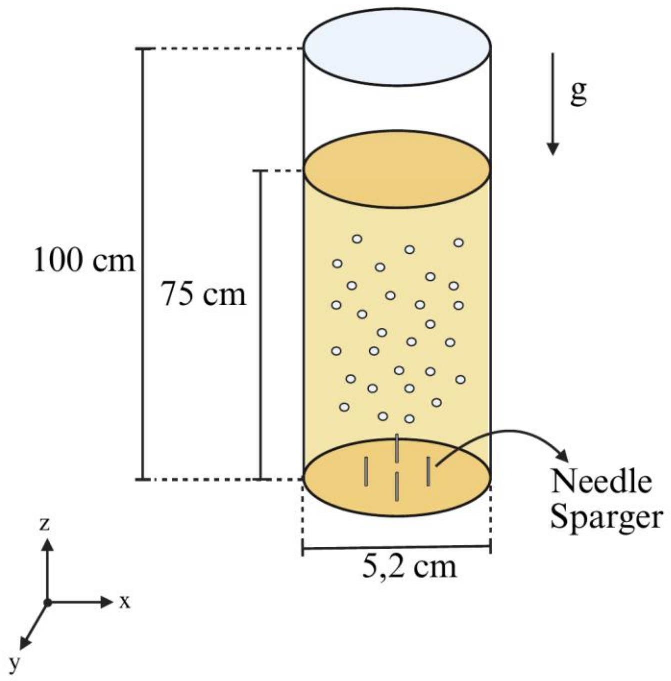

Column of Zhang et al. (2012) ①: 5.2 cm internal diameter, 100 cm high, 75 cm unaerated liquid.

	CO_2 / [BMIM][BF_4] column ①
Liquid phase	[BMIM][BF_4]
Gas phase	CO_2
μ_L [Pa·s]	0.107 (92 × water)
σ [N/m]	0.0436
ρ_L [kg/m³]	1201
He [-]	2.73
Column D_C × H	5.2 cm × 100 cm
Sparger	4 needles
Operating mode	batch
U_G [m/s]	0.0045 – 0.0060
Temperature and pressure	298 K, atmospheric
Flow regime	homogeneous

What is different about it?
Every standard closure was calibrated on air–water. Here the viscosity is 90x higher, so none of them can be assumed to transfer. The regime stays homogeneous.

① Zhang X, Dong H, Huang Y, Li C and Zhang X 2012 Experimental study on gas holdup and bubble behavior in carbon capture systems with ionic liquid Chemical Engineering Journal 209 607–15

Boundary conditions, mesh and numerics

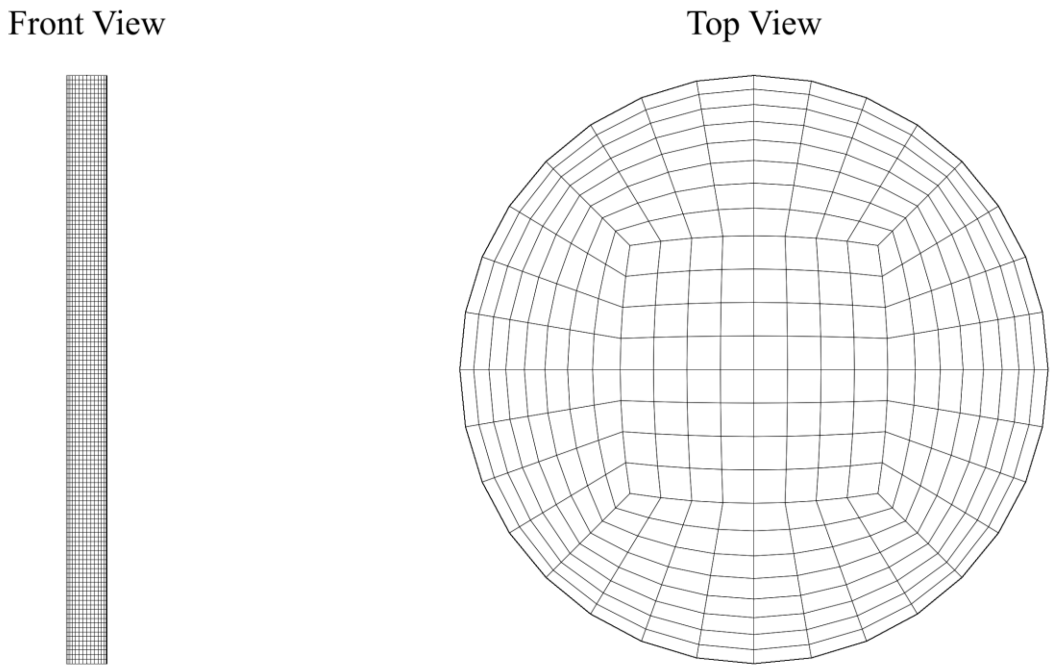

Structured hexahedral mesh of the ionic-liquid column.

Boundary	Treatment
Gas inlet	4 mass source points at the needles
Liquid inlet	none — batch operation
Top	degassing
Walls, liquid	no slip
Walls, gas	free slip
Bubble diameter	Zhang correlation, d_{32}

Mesh

41 600 structured hexahedra, wall-refined; Δx = Δy = 1.63 mm, Δz = 5.77 mm. Mesh and time-step independence verified (backup).

Numerics

PIMPLE, 3 outer / 2 inner correctors; implicit Euler in time; van Leer TVD on the phase fraction. Run to 2100 s, averaged after 20 s.

Results — drag coefficient model assessment

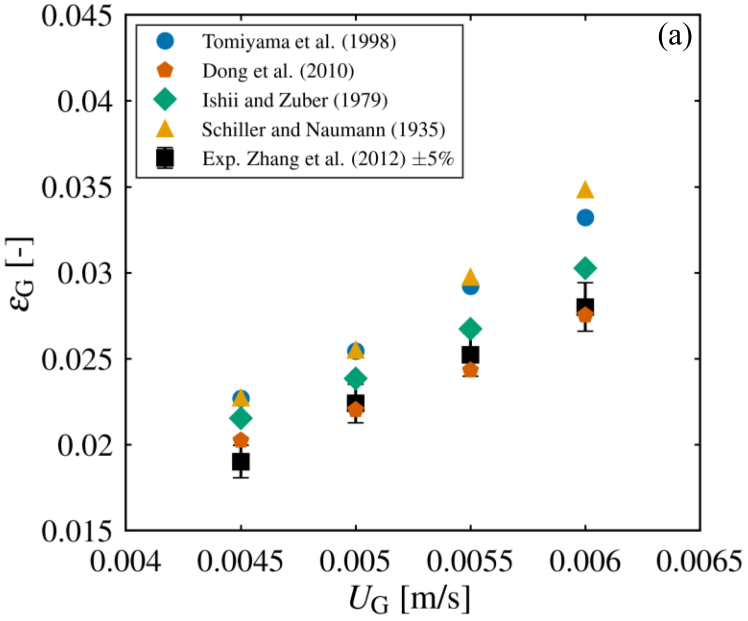

(a) Global gas holdup using differenct drag coefficient models..

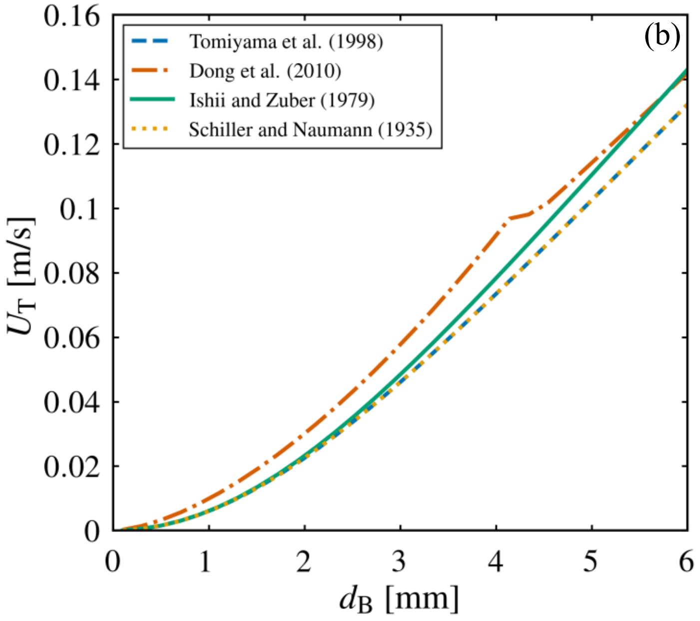

(b) Variation of terminal velocity for different bubble diameters..

Dong et al. (2010)
Deviations between -3.6% and +6.5%; the only correlation without a systematic bias.

Ishii & Zuber (1979)
Deviations between +5.9% and +13.3%; below 10% at three of the four conditions.

Tomiyama / Schiller–Naumann
Mean deviations of +16.9% and +19.0% — the air–water calibration does not transfer.

Difference in bubble terminal velocity results in different gas holdup.

Results — mass transfer in the ionic liquid

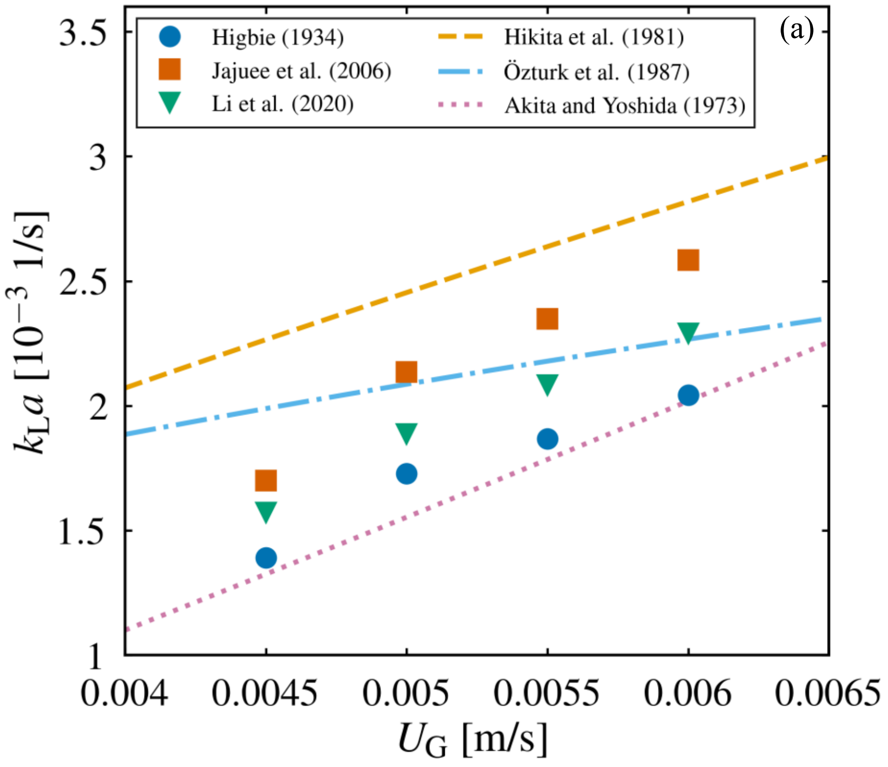

(a) Volume-averaged $k_L a$ against U_G, with the empirical correlations.

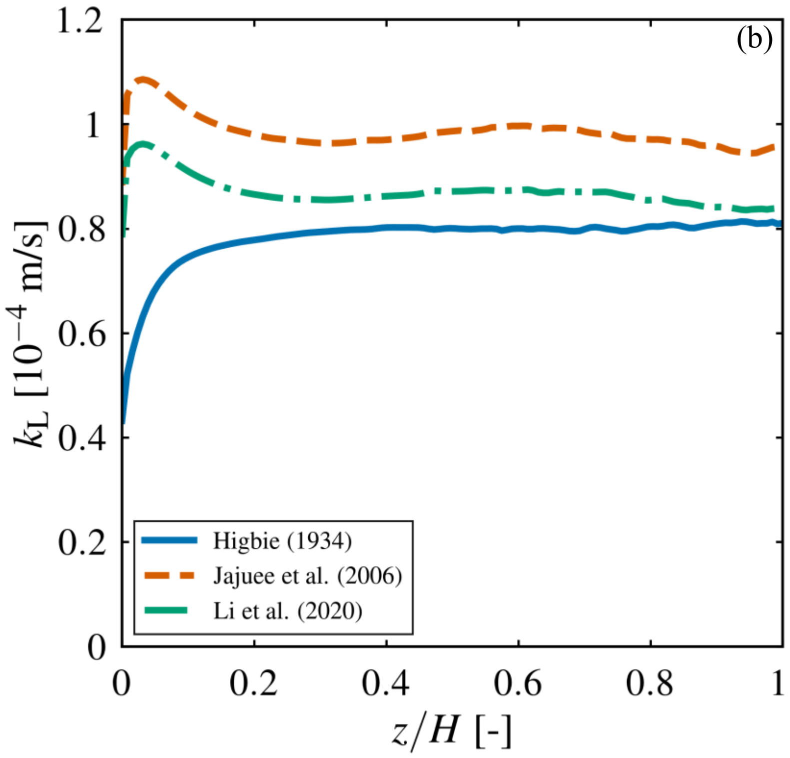

(b) Axial k_L profile at U_G = 0.006 m/s.

Magnitude agrees
All three closures fall inside the spread of the Akita, Hikita and Öztürk correlations.

Location does not
Higbie rises monotonically with the slip velocity; Jajuee and Li peak near the sparger, where ε is highest.

Why it matters
The same volume-averaged $k_L a$ hides a different picture of where the column actually absorbs.

Empirical $k_L a$ correlations in (a): Akita K and Yoshida F 1973 Ind. Eng. Chem. Process Des. Dev. 12 76–80 · Hikita H, Asai S, Tanigawa K, Segawa K and Kitao M 1981 The Chemical Engineering Journal 22 61–9 · Öztürk S S, Schumpe A and Deckwer W-D 1987 AIChE Journal 33 1473–80

Does it generalise? A resolved water benchmark

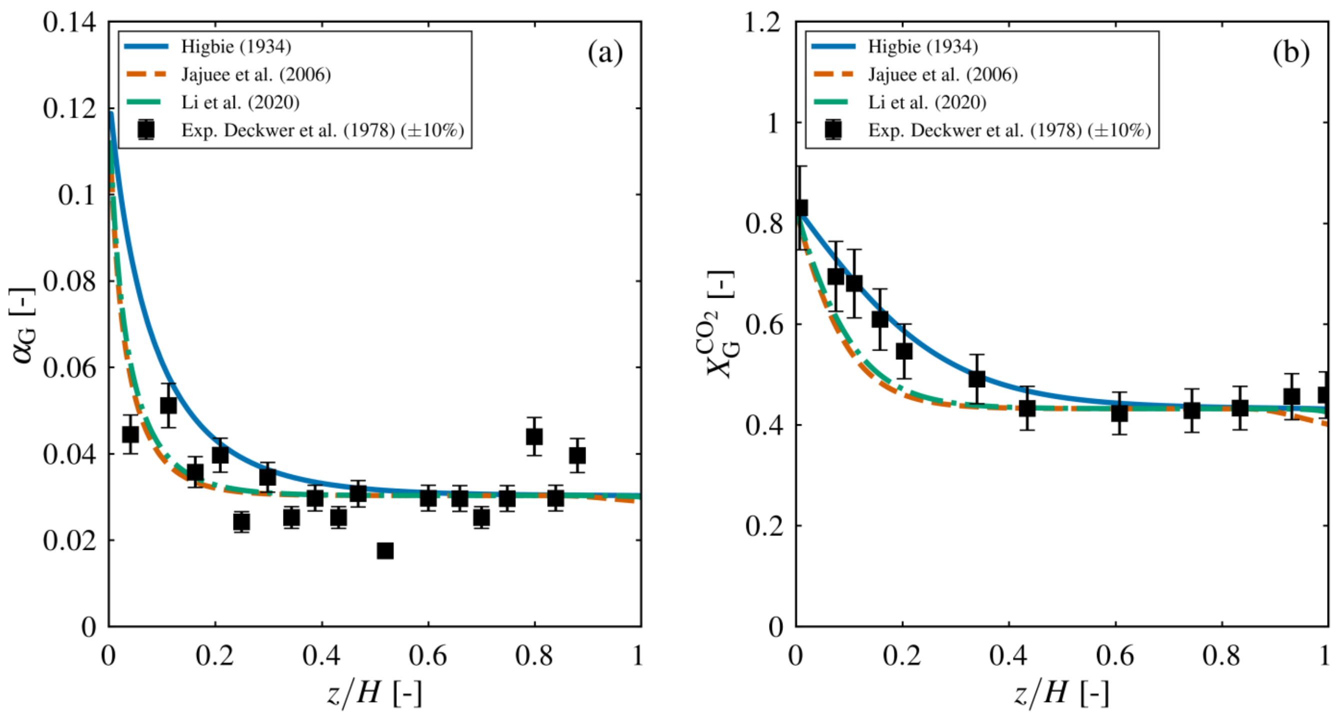

Time-averaged axial (a) gas holdup and (b) CO_2 mole fraction in gas phase against the measurements of Deckwer et al. (1978),

Agreement
Gas holdup within 18–26%, largest at the inlet where the uniform inlet condition; CO_2 mole fraction within 3.7–9.2%.

The benchmark of Deckwer et al. (1978) ②

Liquid / gas	water / air–CO_2
μ_L [Pa·s]	1.166×10^{-3}
Column $D_C \times H$	15 cm × 440 cm
Sparger	sintered plate
Operating mode	cocurrent
U_G [m/s]	0.0275
U_L [m/s]	0.0472
Bubble diameter	2.9 mm, measured

Why this case
It is a CO_2 column with axial profiles of both holdup and gas-phase concentration the only way to test where the closure puts the transfer.

Read it as a generality check
A different liquid, sparger and flow direction, with the closure set left as validated on the ionic liquid.

② Deckwer W-D, Adler I and Zaidi A 1978 A comprehensive study on CO_2-interphase mass transfer in vertical cocurrent and countercurrent gas–liquid flow The Canadian Journal of Chemical Engineering 56 43–55

Results — impact of bubble-induced turbulence

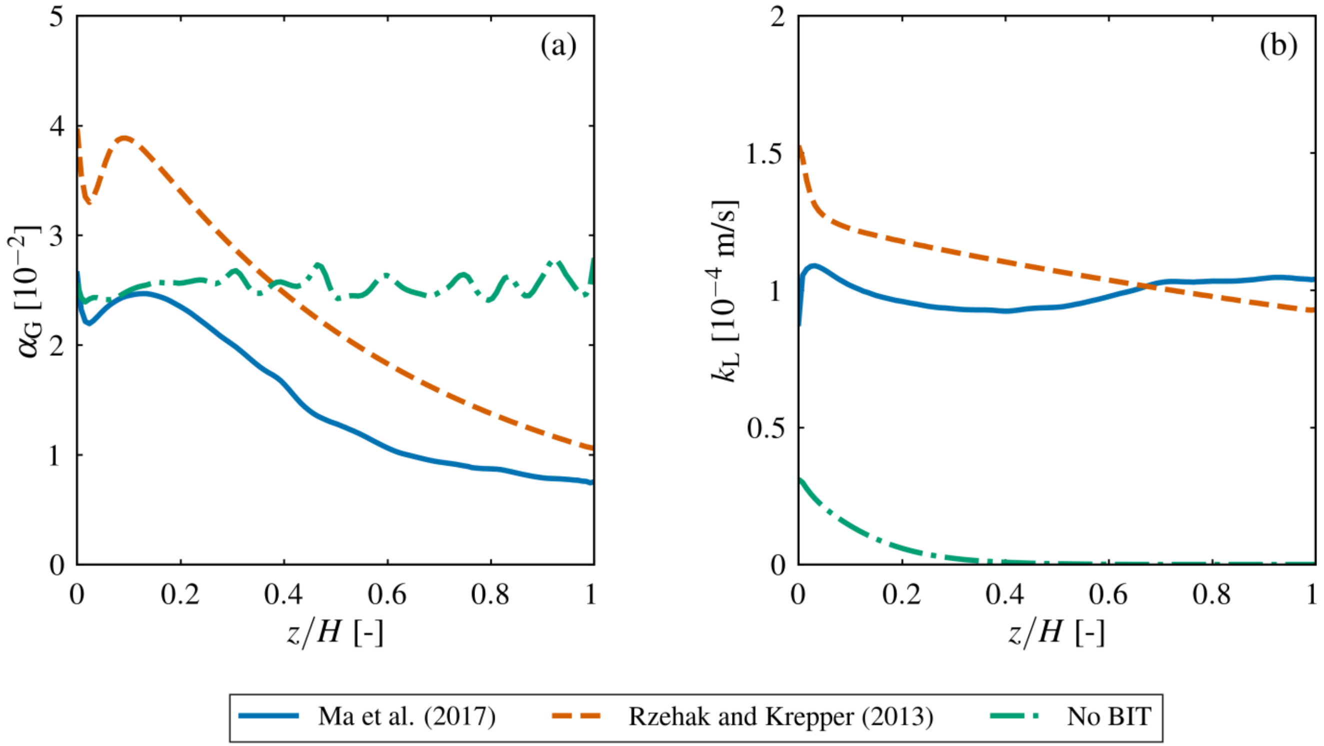

(a) Gas holdup and (b) k_L axial profiles comparing BIT models

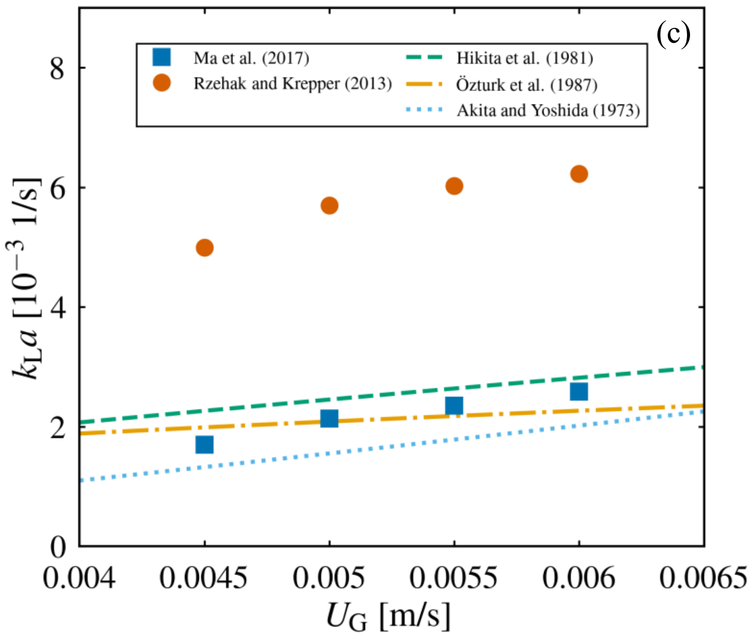

(c) Volume-averaged $k_L a$ against U_G.

Without BIT
ε collapses, $k_L a$ falls to negligible levels and Higbie shows an unphysical rise near the top.

Rzehak & Krepper ⑮
All the drag work becomes turbulent kinetic energy: ε and $k_L a$ are inflated above the correlation band.

Ma et al. ⑭ †
The $\min(0.18\, Re_B^{0.23}, 1)$ factor damps the source term proviginf the best agreement with the correlations.

⑭ *Ma T, Santarelli C, Ziegenhein T, Lucas D and Fröhlich J 2017 Direct numerical simulation–based Reynolds-averaged closure for bubble-induced turbulence Physical Review Fluids 2 034301*
⑮ *Rzehak R and Krepper E 2013 Closure models for turbulent bubbly flows: a CFD study Nuclear Engineering and Design 265 701–11*

Results — impact of the operating mode

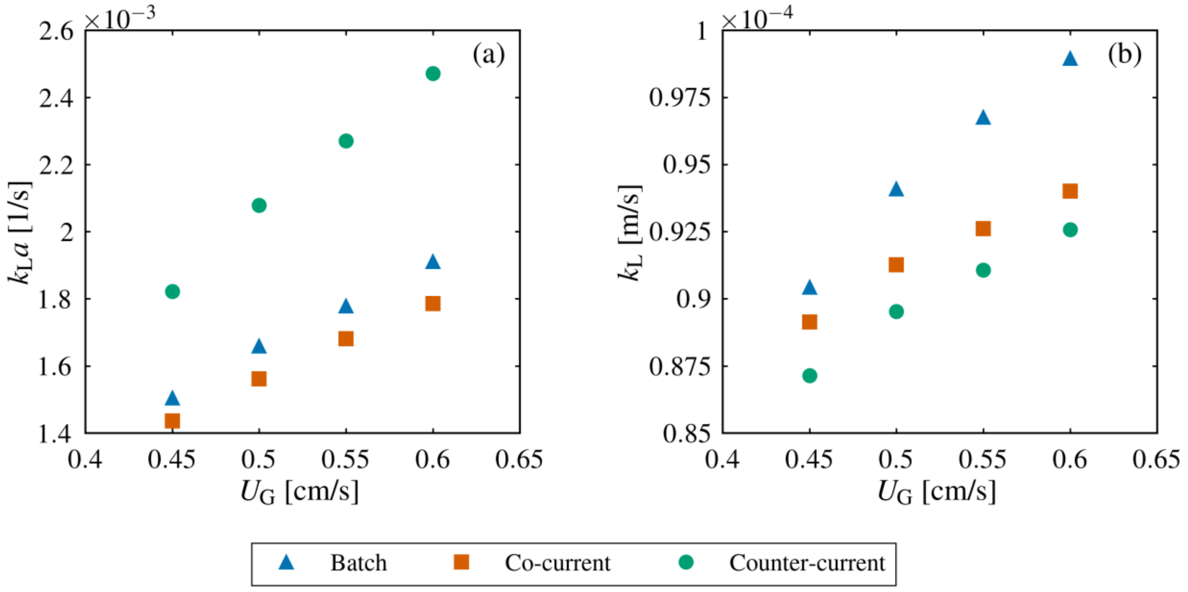

(a) $k_L a$ and (b) k_L against U_G for the three modes.

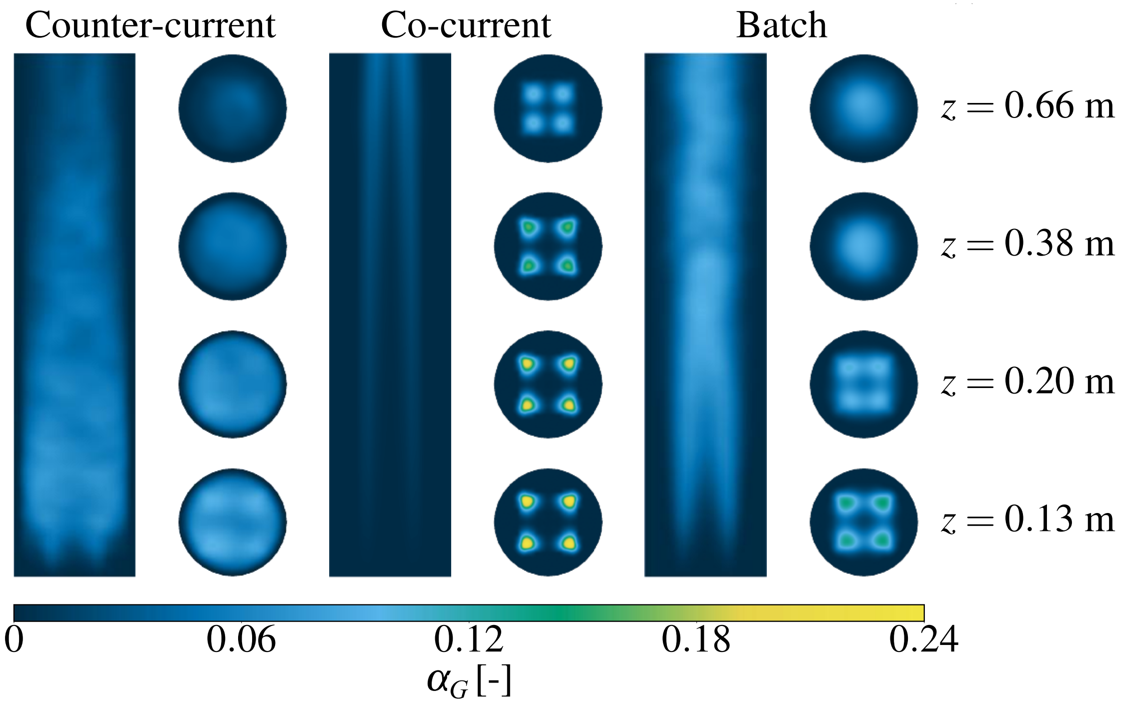

(c) Void fraction contour slices.

Counter-current gives the highest $k_L a$
The opposing liquid flow retains the bubbles, the gas holdup and provides larger interfacial area.

Batch gives the highest k_L
Predicted values are larger than those for Counter and Co-current.

Contour Illustrates
Opposing flows causes higher dispersion of gas phase in the column increasing interfacial area.

U_L = 0.03 m/s, Jajuee k_L closure with the Ma BIT source.

Conclusions

Drag first

Air–water drag correlations overestimate the gas holdup in ionic liquids; Dong's IL-fitted correlation stays within -3.6% to +6.5%. Closure selection precedes any mass transfer analysis.

Global agreement is not local agreement

All three k_L closures land inside the empirical band, but Higbie is slip-driven and Jajuee/Li are ε-driven they disagree on where in the column the transfer happens.

BIT need to account for viscosity

Absence and overestimation are equally harmful. Ma's Re_B-corrected closure reproduces the correlations; Rzehak's, calibrated on air–water, inflates ε and $k_L a$ and do not accounts viscous liquids.

Counter-current maximises $k_L a$

Batch gives the highest k_L, but counter-current operation retains the bubbles, raises the holdup and therefore the interfacial area.

Outlook

Extending the closure assessment to other ionic liquids, to the transition and heterogeneous regimes, and to reactive solvents, where the liquid-film reaction has to be resolved as well.

Ministero dell'Università e della Ricerca | FIS | POLITECNICO MILANO 1863 | DEPARTMENT OF ENERGY

Thank you for your attention

Acknowledgment

This work has been financed by the Italian Ministry of University and Research (Ministero dell'Universita. e della Ricerca) within the FIS2 call. In particular, This work has been conducted within the AURIGA ("Unveiling the RIddles of GAs liquid fluid dynamics: towards novel carbon dioxide absorption systems") project. Project number FIS-2023-00204, CUP D53C25000730001, funded within the FIS2 call (Decreto Direttoriale n. 1236 del 1-08-2023).

Contatti

vitoraugusto.regert@polimi.it

www.polimi.it

Backup

B

Backup — mesh independence

Mesh	Cells	Axial	Radial	Global gas holdup
Coarse	18 000	100	12	2.22%
Medium †	41 600	130	16	2.24%
Fine	80 000	160	20	2.25%

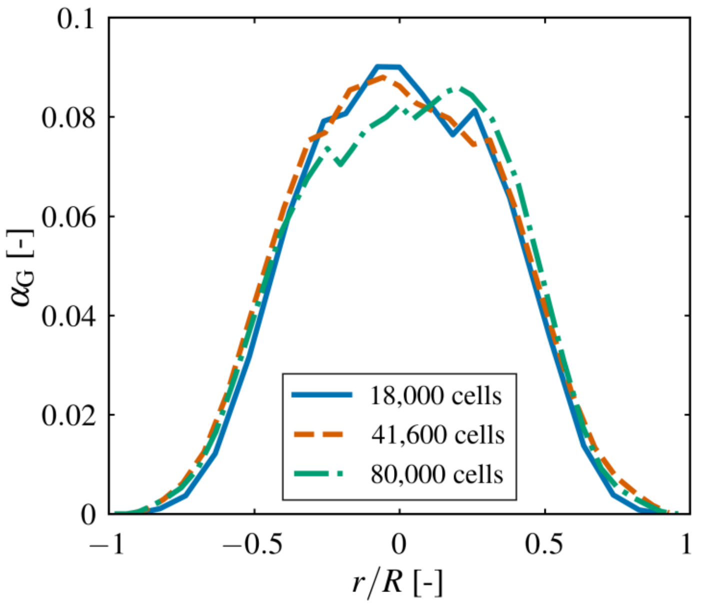

Radial gas-holdup profiles at U_G = 0.006 m/s; the global holdup changes by 0.03 percentage points across the three grids, so the medium mesh (41 600 cells) is retained for all production runs.

Backup — time-step independence

Δt [s]	Max Courant number	Global gas holdup
0.003 †	0.316	2.24%
0.005	0.524	2.23%
0.008	0.828	2.22%

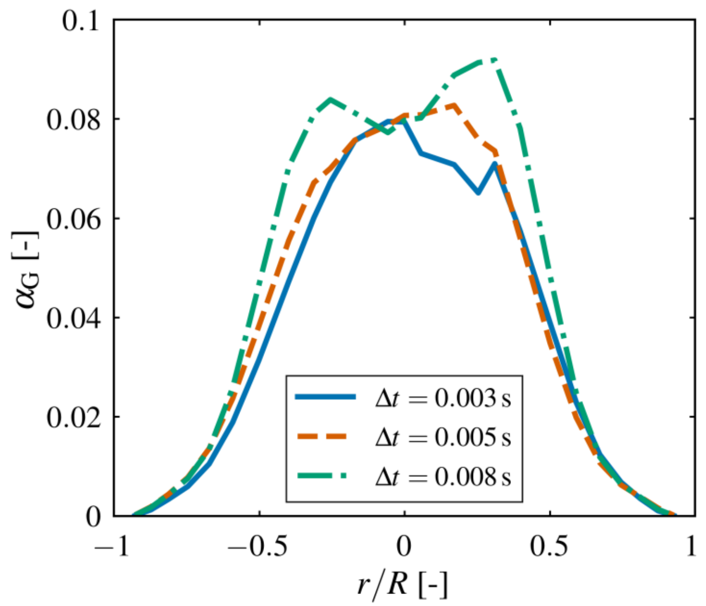

Radial gas-holdup profiles for three time steps, with the time-averaged maximum Courant number verified in each case; the global holdup varies by 0.02 percentage points.

Backup — discretisation schemes

Term	Scheme
Time derivative	Euler, implicit first order
Phase fraction convection	van Leer TVD, bounded
Momentum convection	limited linear, bounded second order
Turbulence convection	limited linear, bounded second order
Species convection	limited linear, bounded second order
Diffusion	corrected central differences
Pressure	GAMG, tolerance 1e-8
U, k, ω, Y	smooth solver, Gauss–Seidel

Backup — physical properties

Property	[BMIM][BF_4] – CO_2 (298 K)	Water – CO_2/air (287 K)
ρ_L [kg/m³]	1201	998
ρ_G [kg/m³]	1.8074	1.85
μ_L [Pa·s]	0.1069	1.166×10^{-3}
μ_G [Pa·s]	1.49×10^{-5}	1.4396×10^{-5}
σ [N/m]	0.0436	0.073
D [m²/s]	3.8×10^{-10}	1.466×10^{-9}
He [–]	2.73	0.96

Sources: Zhang et al. (2012) and Anthony et al. (2005) for the ionic-liquid system; Rzehak & Krepper (2016) for the water system.

Why Ma's closure wins at high viscosity

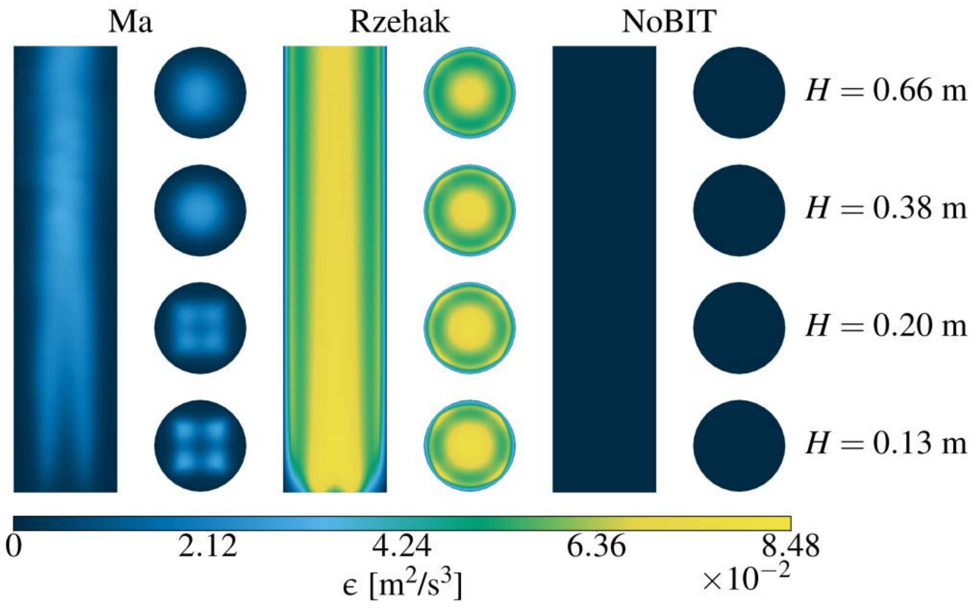

(a) Time-averaged ε field.

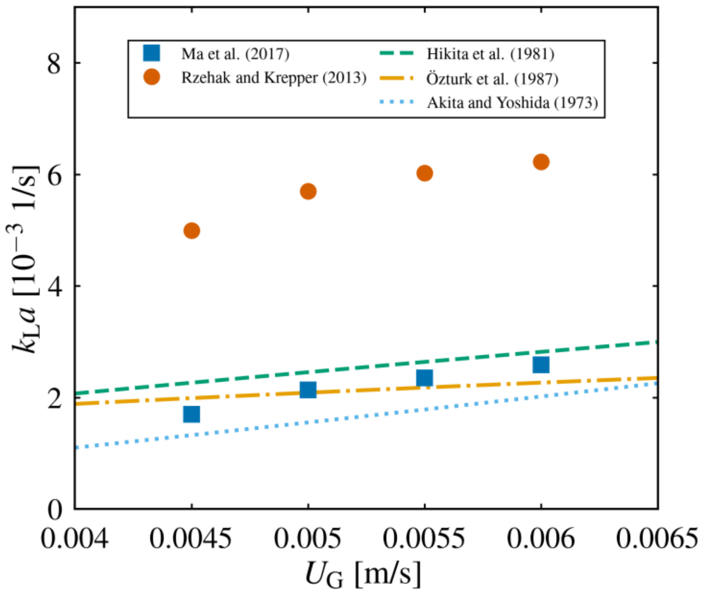

(b) $k_L a$ against U_G with the correlations.

$$\min(0.18\, Re_B{}^{0.23}, 1) \ll 1 \quad \text{for} \quad Re_B = O(1)$$

Rzehak & Krepper ⑮

No Re_B correction: ε and $k_L a$ are inflated well above the correlation band.

BIT closures without an explicit viscosity correction should not be transferred across viscosity regimes.

⑭ Ma T, Santarelli C, Ziegenhein T, Lucas D and Fröhlich J 2017 Direct numerical simulation–based Reynolds-averaged closure for bubble-induced turbulence Physical Review Fluids 2 034301
⑮ Rzehak R and Krepper E 2013 Closure models for turbulent bubbly flows: a CFD study Nuclear Engineering and Design 265 701–11

Backup — nomenclature

α_K	volume fraction of phase K	d_B, d_{32}	bubble and Sauter mean diameter
ρ_K, μ_K	density, dynamic viscosity	$C_D, C_L, C_{\mathrm{VM}}$	drag, lift, virtual-mass coefficients
$\boldsymbol{u}_K, \boldsymbol{u}_r$	phase velocity, relative velocity	k, ω, ϵ	turbulence quantities
$\bar{\tau}_K$	phase stress tensor	$k_L a$	volumetric mass transfer coefficient
$\boldsymbol{M}_K$	interphase momentum exchange	Re_B, Mo, Eo	bubble Reynolds, Morton, Eötvös
$\Gamma_K, \Gamma_K{}^i$	mass and species source	He	dimensionless Henry constant of CO_2